MEASUREMENT OF THE GAS-SIDE MASS TRANSFER COEFFICIENT BY LIQUID JET

KAKUSABURO ONDA, EIZO SADA and MINORU NAGASAKA

Department of Chemical Engineering

(Received May 28, 1965)

Introduction

Since a new experiment of gas absorption by liquid jet by Matsuyama[8] has been carried out, many investigators used liquid jet for gas absorption experiments because of its accuracy in the experimental results and convenience. For the experiments in physical as well as chemical absorption, the liquid jet was used to determine the diffusion coefficients[10], interfacial resistance[2)14)] and the reaction rates[4)5)9)15)]. In almost all the experiments in the past, the gas was stagnant and the liquid flowed down. The amount of mass transfer was measured by the decrease of volume of the gas chamber or by the change of the liquid concentration. Of course, both of them used pure gases, and carried out in the state of no interfacial resistance. In the case of the generation or absorption of heat is small as in the physical gas absorption, the results by the experiment have coincided well with the theoretical values by the penetration theory. But in the chemical absorption where considerable heat exchange takes place, the change of temperature with the concentration change will be hasty near the interface. This hasty temperature change causes the uncertainties of the derived values of reaction rate, diffusivity etc. from the differential equations which was constructed considering only the mass transfer. This is the reason why the dilute gas mixture is always used in the chemical gas absorption experiments. In this case, the gas-side mass transfer resistance becomes appreciable and thus the gas-side mass transfer coefficient (k_G) by liquid jet experiment was investigated in this paper.

There is only one report by Hatch and Pigford[5] about k_G by liquid jet expriment. They flowed gas tangentially against liquid jet and investigated the dependence of k_G on gas concentration, gas velocity, diffusivity etc. and have derived an empirical formula for it. But it has no theoretical guarantee and no generalization.

The cylindrical coordinates was used to derive the theoretical equation. The agreement of the experimental results with the theoretical was investigated. The system used are H_2-H_2O, N_2-H_2O, O_2-H_2O and N_2-NH_4OH soln.

One of the assumptions taken in the derivation of the theoretical equation is that $v_G=v_L$, but this condition is hardly carried out in the ordinary gas absorption experiments by liquid jet. Then experiments with $v_G \neq v_L$ was also carried out and a convenient empirical equation was presented.

Theory

In general, the mechanism of gas absorption by the liquid jet is taken to be

unsteady state, and the penetration theory by Higbie is applied. In the experiments of the liquid side mass transfer coefficient (k_L), diameter of the liquid jet is very large in comparison with the diffusing distance in the liquid phase. Then the assumption that the interface is plane will be plausible. But diffusing distance in gas is large in comparison with jet diameter and in this case it is unreasonable to consider that the liquid surface (interface) is plane. The diffusing distance in gas amounts to several hundred times ($\fallingdotseq\sqrt{D/D'}$) as large as that in liquid. In order to get k_G theoretically, it is necessary to consider that the interface is cylindrical and that the theoretical equation is derived by cylindrical coordinates.

On deriving the theoretical equation, the following three assumptions were made.

Assumptions:

1. The liquid velocity (v_L) is uniform in the direction of the flow and the radius.

2. The gas velocity (v_G) is equal to the liquid velocity and uniform in the direction of the flow and the radius.

3. The liquid-side resistance and the interfacial resistance are disregarded. That is, in the vaporization experiments, pure H_2O was used and in the desorption experiments NH_4OH soln. which is considered that the liquid-side resistance is small, was used.

If the diffusion occurs only in the direction of the radius, the diffusional equation based upon the unsteady state is written as following.

$$\frac{\partial c}{\partial t}=\frac{1}{r}\cdot\frac{\partial}{\partial r}\left(rD\frac{\partial c}{\partial r}\right) \tag{1}$$

The initial and boundary conditions are

$$\left.\begin{array}{lll} r>a & t=0 & c=c_0 \\ r\leqq a & t=0 & c=c_1 \\ r\to\infty & t>0 & c=c_0 \end{array}\right\} \tag{2}$$

And the solution[3] for Eq. (1) and (2) is

$$\frac{c-c_0}{c_1-c_0}=1+\frac{\pi}{2}\int_0^\infty\frac{\exp(-Du^2t)[J_0(ur)Y_0(ua)-J_0(ua)Y_0(ur)]du}{u[J_0^2(ua)+Y_0^2(ua)]} \tag{3}$$

where J_0 and Y_0 are the first and second kind of Bessel function respectively. The absorption rate N_i [mole/cm^2·sec] at any time t [sec] is given

$$N_i=-D\left(\frac{\partial c}{\partial r}\right)_{r=a}=\frac{4(c_1-c_0)}{\pi^2a}\int_0^\infty\frac{\exp(-Du^2t)du}{u[J_0^2(ua)+Y_0^2(ua)]} \tag{4}$$

And the mean absorption rate N [mole/cm^2·sec] at the time $t=0\sim t$ [sec] is given

$$N=\frac{1}{t}\int_0^t N_i\,dt=\frac{4(c_1-c_0)}{\pi^2at}\int_0^\infty\frac{[1-\exp(-Du^2t)]du}{u^3[J_0^2(ua)+Y_0^2(ua)]}$$

Putting $au = \lambda$, the above equation becomes as following,

$$N = \frac{4\,a(c_1 - c_0)}{\pi^2 t} \int_0^\infty \frac{\left[1 - \exp\left(-\frac{Dt}{a^2} \cdot \lambda^2\right)\right] d\lambda}{\lambda^3 [J_0^2(\lambda) + Y_0^2(\lambda)]} \tag{5}$$

Eq. (5) is the theoretical equation of the absorption rate from the cylindrical surface by the penetration theory. Further, when the absorption rate is expressed as the product of k_G by the difference of the concentration, it becomes

$$N = k_G (c_1 - c_0) \tag{6}$$

When Eq. (5) is compared with Eq. (6), Eq. (7) is derived

$$k_G = \frac{4\,a}{\pi^2 t} \int_0^\infty \frac{\left[1 - \exp\left(-\frac{Dt}{a^2} \cdot \lambda^2\right)\right] d\lambda}{\lambda^3 [J_0^2(\lambda) + Y_0^2(\lambda)]} \tag{7}$$

Rearranging of Eq. (7),

$$\frac{k_G a}{D} = \frac{4}{\pi^2} \cdot \frac{a^2}{Dt} \int_0^\infty \frac{\left[1 - \exp\left(-\frac{Dt}{a^2} \cdot \lambda^2\right)\right] d\lambda}{\lambda^3 [J_0^2(\lambda) + Y_0^2(\lambda)]} \tag{8}$$

Taking as $(Re) = aV\rho/\mu$, $(Sc) = \mu/\rho D$, $(Sh) = k_G a/D$ and $a/t = V$, Eq. (8) can be written as Eq. (9),

$$(Sh)_{(9)} = \frac{4}{\pi^2} \cdot (Re)(Sc) \int_0^\infty \frac{[1 - \exp(-\lambda^2/(Re)(Sc))] d\lambda}{\lambda^3 [J_0^2(\lambda) + Y_0^2(\lambda)]} \tag{9}$$

On the other hand, when the absorption occurs on the plane surface, k_G is given in Eq. (10),

$$k_G = \frac{2}{\sqrt{\pi}} \cdot \sqrt{\frac{D}{t}} \tag{10}$$

Eq. (10) is rearranged as Eq. (8) and we get,

$$(Sh)_{(11)} = \frac{2}{\sqrt{\pi}} \{(Re)(Se)\}^{1/2} \tag{11}$$

On the log-log paper with $(Sh) = k_G a/D$ on the abscissa and $(Re)(Sc) = a^2/Dt$ on the ordinate, Eq. (9) and Eq. (11) were plotted in Fig. 1. Eq. (11) becomes straight of which slope is 1/2. Eq. (9) is curve with the asymptote of Eq. (11). It is clear from Fig. 1 that when the value of $(Re)(Sc) = a^2/Dt$ is small the difference becomes very large. That is, the

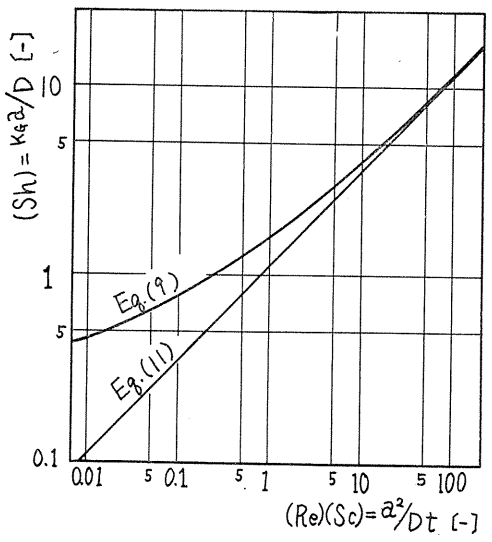

FIG. 1. Theoretical curves for Eq. (9) and Eq. (11).

ratios $(Sh)_{(9)}/(Sh)_{(11)}$ are 1.05 at $(Re)(Sc)=100$, 1.39 at $(Re)(Sc)=1$ and 2.19 at $(Re)(Sc)=0.1$.

Experimental apparatus and Procedure

The schematic diagram of the apparatus is shown in Fig. 2 and the details of the vaporization (or desorption) chamber is shown in Fig. 3. The diameter and other dimensions of the liquid nozzle are described in Fig. 4. The rate of mass transfer were calculated by the determination of H_2O in gas or NH_3 in gas by P_2O_5 or H_2SO_4 soln. respectively.

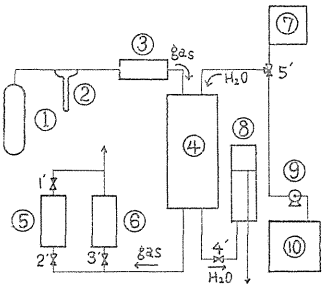

① gas bomb
② flow meter
③ dryer
④ vaporization (or desorption) chamber
⑤ P_2O_5 tube (or H_2SO_4 soln)
⑥ packed tube
⑦ head tank
⑧ liquid level controller
⑨ straw pump
⑩ reservoir 1′~5′ cock

FIG. 2. Schematic diagram of experimental apparatus.

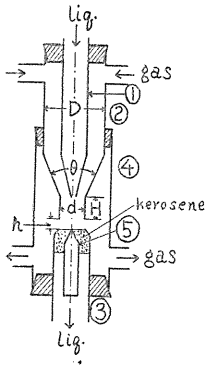

① liquid nozzle
② gas nozzle
③ receiver
④ gas mantle
⑤ glass rod

$D=1.73$ cm $d=0.82$ cm
$H=2.17$ cm $h=5$ mm
$\theta=15°$

FIG. 3. Details of vaporization (or desorption) chamber.

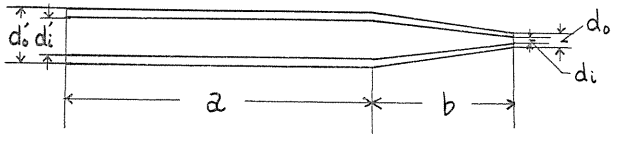

nozzle No.	a (cm)	b (cm)	d_0' (cm)	d_i' (cm)	d_0 (cm)	d_i (cm)
1	10.9	3.1	0.99	0.76	0.109	0.050
2	9.1	2.8	1.00	0.76	0.123	0.057
3	10.5	3.7	0.99	0.76	0.124	0.070
4	8.4	3.2	0.90	0.65	0.125	0.075
5	10.5	3.8	0.99	0.76	0.132	0.085
6	7.7	3.5	0.91	0.66	0.129	0.092
7	10.6	3.6	1.00	0.76	0.153	0.100

(d_i equals to nozzle diameter (a))

FIG. 4. Liquid nozzle (glass).

Experimental results and Discussion

As the preparatory experiments, the determination of the liquid-side mass transfer coefficient k_L of CO_2 and SO_2 in H_2O using pure CO_2 and SO_2, were carried out. The results are shown in Fig. 5, the diffusivities and the solubilities to calculate k_L are tabulated in Table 1. The coincidence of the results with the theoretical is satisfactory. From this coincidence, the gas flow has no influence on k_L and the apparatus can be used without serious error.

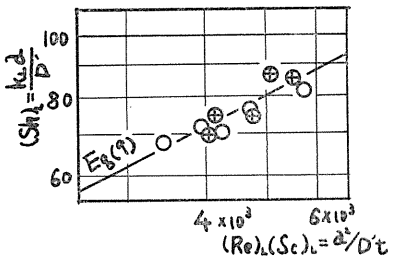

—: theoretical curve (Eq. (9))
○: CO_2-H_2O
⊕: SO_2-H_2O

FIG. 5. Liquid-side mass transfer coefficient for CO_2- and SO_2-H_2O systems.

1. Vaporization of water into H_2, N_2 and O_2

The liquid was distilled water and the gases were above 99% purity respectively. The temperature range and the nozzle diameter are shown in Table 2.

TABLE 1. Diffusivitities and Solubilities (25°C 1 atm)

System	Diffusivity (cm^2/sec)	Solubility (mole/cc)
CO_2-water	1.96×10^{-5} [12]	3.39×10^{-5} [11]
SO_2-water	1.7×10^{-5} [13]	1.34×10^{-3} [7]

TABLE 2. Nozzle diameter and Temperature range

System	Nozzle dia. (cm)		Temp. range (°C)
H_2-H_2O	0.050	0.070	18~25
	0.085	0.100	
N_2-H_2O	0.057	0.075	25~30
	0.100		
O_2-H_2O	0.050	0.057	20~30
	0.085	0.100	

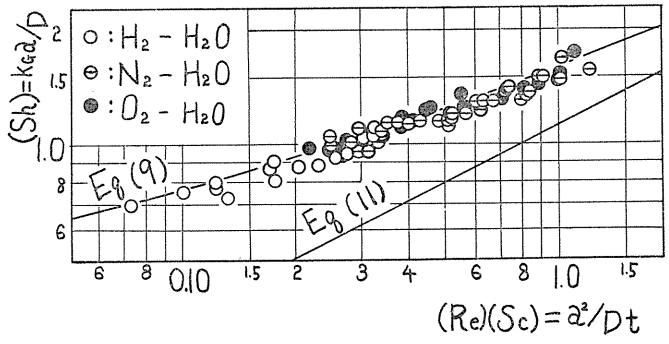

FIG. 6. Vaporization of water into H_2, N_2 and O_2.

The results were plotted in Fig. 6. The experimental results agreed well with the theoretical curve (Eq. (9)).

The diffusivity for H_2-H_2O is about fourth as large as that for N_2- and O_2-H_2O, and the results for H_2-H_2O are located at the left side in Fig. 6. This showes clearly that the jet surface must be considered as a cylinder surface in calculating k_G.

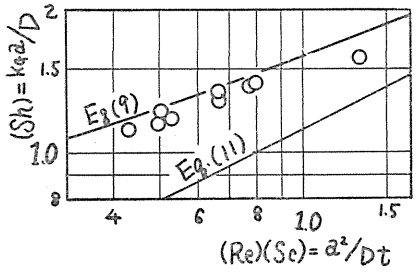

FIG. 7. Desorption of NH_3 from NH_4OH soln. to N_2.

The fact that the dependences of k_G on the nozzle diameter and temperature coincide with the theoretical value, shows that the applicability of this procedure and apparatus is reasonable.

2. Desorption of NH_3 from NH_4OH soln. into N_2

The liquid was 0.495 N and 1.735 N NH_4OH soln. The nozzle diameter was 0.092 cm and the temperature was 21.5~23.0°C. The results were plotted in Fig. 7. In this system, the liquid-side resistance should be considered. W. Vielstich[18] has derived the equation applicable to the system where both resistances are present, but his equation is based on the assumption that the interface is plane. For convenience, however, the resistance in each phase is discussed with his equation as follows:

The desorption rate is

$$N=2\sqrt{\frac{D'}{\pi t}}\cdot\frac{1}{1+\alpha'\sqrt{D'/D}}(\alpha' c_0-c_0') \tag{12}$$

where α' is Ostwald's absorption coefficient and c_0' is solute concentration in liquid phase. On the other hand, with no gas-side resistance the mean desorption rate is

$$N=2\sqrt{\frac{D'}{\pi t}}(\alpha' c_0-c_0') \tag{13}$$

It is understood from Eq. (12) that when both the gas- and liquid-side resistance are present, the mass transfer coefficient becomes to $\{1/(1+\alpha'\sqrt{D'/D})\}$ times. That is, the resistance becomes to $(1+\alpha'\sqrt{D'/D})$ times. When the gas such as N_2 or O_2 is desorbed from water, $\alpha'\sqrt{D'/D}\ll 1$, then $1+\alpha'\sqrt{D'/D}\fallingdotseq 1$ and the gas-side resistance can be negligible. For CO_2 desorbed from water, the value of $(1+\alpha'\sqrt{D'/D})$ becomes to 1.01. About 1% of the total resistance belongs to the gas-side resistance. From the accuracy of the experiment, this value of error (=1%) is negligible. The solubility of NH_3 to water, however, is very large, the value of α' is about 1500 and the value of $(1+\alpha'\sqrt{D'/D})$ is nearly equal to 13. This shows that the liquid-side resistance is about 8% of the total resistance and that the gas-side resistance is about 92%. The experimental results in Fig. 7 are calculated with the assumption that all the resistances exist in the gas phase. The experimental results are lower than the theoretical value by about 5%. This discrepancy seems to be due to the ignorance of the liquid-side resistance. Therefore, it is considered that the results agree well with the theoretical value.

3. Diffusivities and Jet diameters

The diffusivities in the literatures for various systems are tabulated in Table 3. The diffusivities of N_2-H_2O and N_2-NH_3 are calculated from the experimental values for air. And the diffusivity of O_2-H_2O was calculated by the empirical equation[16]. The diffusivities used are tabulated in Table 4.

In calculating the results, the diameter of the liquid nozzle was taken as the diameter of the liquid jet. The jet diameter was slightly different from nozzle diameter. The difference between these two diameters was about 5% as shown in Fig. 8.

4. For the case of $v_G \neq v_L$ in the vaporization experiments

In the case in which the liquid velocity was not equal to the gas velocity, the experiments were carried out. The system used was N_2-H_2O. The gas velocity was twice, half times and quarter times as fast as the liquid velocity respectivoly. The results are plotted in Fig. 9, 10 and 11. In these cases, the various contact times can be taken. That is, there are the contact times calculated from the gas velocity, the liquid velocity, the mean velocity of the gas and liquid and so on. The results based on the gas velocity or the liquid are plotted in Fig. 9~11. But the experimental results in both methods do not agree with the theoretical curve (Eq. (9)). The both results are located symmetrically to the theoretical

TABLE 3. Diffusivities in the Literature

System	Diffusivities (cm^2/sec)	
H_2-H_2O	0.850	20°C 1 atm[17]
air-H_2O	0.220	0°C 1 atm[6]
air-NH_3	0.198	0°C 1 atm[1]

TABLE 4. Diffusivities (20°C 1 atm)

System	Diffusivities (cm^2/sec)	Index of temperature
H_2-H_2O	0.850	1.75
N_2-H_2O	0.243	1.75
O_2-H_2O	0.246	
N_2-NH_3	0.222	1.833

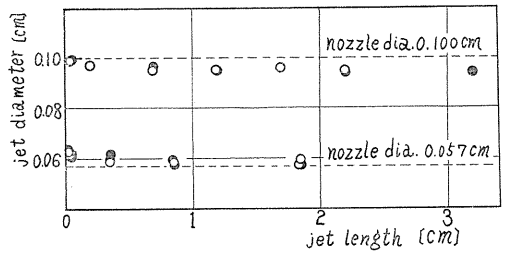

nozzle dia.	mark	liq. flow rate
0.100 cm	○	69 cc/min
	●	120
0.057	○	29
	●	39

FIG. 8. Measurement of jet-diameter vs. various jet-length.

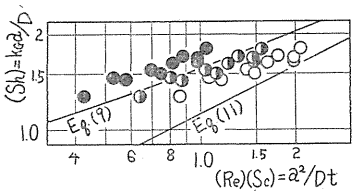

○ calculated values on the basis of v_G
◑ calculated values on the basis of $(v_G+v_L)/2$
● calculated values on the basis of v_L

FIG. 9. Relation of (Sh) vs. (Re) (Sc) in the case of $v_G=2\,v_L$.

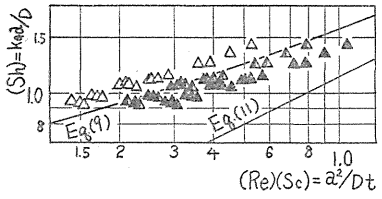

△ calculated values on the basis of v_G
◭ calculated values on the basis of $(v_G+v_L)/2$
▲ calculated values on the basis of v_L

FIG. 10. Relation of (Sh) vs. (Re) (Sc) in the case of $v_G=1/2\,v_L$.

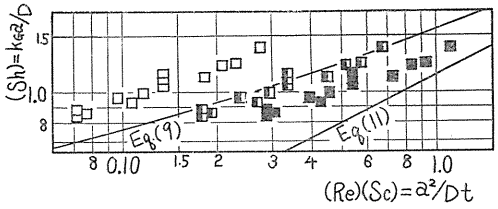

□ calculated values on the basis of v_G
◧ calculated values on the basis of $(v_G+v_L)/2$
■ calculated values on the basis of v_L

FIG. 11. Relation of (Sh) vs. $(Re)(Sc)$ in the case of $v_G=1/4\,v_L$.

curve. If the slip occurs perfectly at the interface with no resistance and the velocity distribution in each phase is uniform, the experimental results should coincide with the theoretical values based on the gas velocity. The liquid velocity distribution may be uniform, but it seems that the gas near the interface flows at the liquid velocity rather than the gas velocity of bulk flow. So there occurs the gas velocity gradient near the interface. In this case, it is reasonable that the contact time should be calculated as the function of the gas and liquid velocity. As a trial, it is assumed that the velocity is taken as the arithmetic mean of the gas and liquid velocity. The recalculated results based on this assumption are shown in Fig. 9~11. These values are agreed well with the theoretical curve (Eq. (9)). In the case of $v_G \neq v_L$, it is easy to calculate k_G by this relation.

Conclusion

1. The vaporization of water into H_2, N_2 and O_2 and the desorption of NH_3 from NH_4OH soln. are investigated by the liquid jet. The results are agreed well with the theoretical equation based on the cylindrical coordinates. The equation is,

$$(Sh)_{(9)} = \frac{4}{\pi^2}(Re)(Sc)\int_0^\infty \frac{[1-\exp(-\lambda^2/(Re)(Sc))]d\lambda}{\lambda^3[J_0^2(\lambda)+Y_0^2(\lambda)]} \qquad (9)$$

2. The case in which both gas- andliquid-side resistances are present, that is the desorption of NH_3 from NH_4OH soln., was discussed qualitatively.

3. The case in which the liquid velocity was not equal to the gas velocity, was studied. When the ratio of the gas velocity to the liquid velocity is between 2 and 1/4, it was confirmed that k_G was approximately calculated by Eq. (9), using the velocity calculated as the arithmetic mean of the gas and liquid velocities.

Nomenclature

a : radius of liquid jet [cm]
c : concentration of solute in gas phase [mole/cc]
c_1 : initial solute concentration in gas phase [mole/cc]
c_0 : solute concentration in gas phase at the interface [mole/cc]
D : diffusivity in gas phase [cm²/sec]
D': diffusivity in liquid phase [cm²/sec]
k_G : gas-side mass transfer coefficient [cm/sec]
k_L : liquid-side mass transfer coefficient [cm/sec]
N : mean absorption (or desorption) rate [mole/cm²·sec]
N_i: absorption (or desorption) rate [mole/cm²·sec]
Re: Reynolds number ($=aV\rho/\mu$) [−]
r : radial distance from axis of liquid jet [cm]
Sc: Schmidt number ($=\mu/\rho D$ or $\mu'/\rho' D'$) [−]
Sh: modified Sherwood number $\left(=\frac{k_G a}{D} \text{ or } \frac{k_L a}{D'}\right)$ [−]
t : time [sec]
v_G : mean gas velocity [cm/sec]
v_L : mean liquid velocity [cm/sec]
ρ : density [gm/cc]
μ : viscosity [gm/cm·sec]

Literature cited

1) Arnold, J. H.: Ind. Eng. Chem., **22**, 1091 (1930).
2) Chiang, S. H. L. Toor: A. I. Ch. E. Journal, **5**, 165 (1959).
3) Crank, J.: "The Mathematics of Diffusion" Oxford (1956).
4) Edward, G., R. Robertson, F. Rumford and J. Thomson: Trans. Inst. Chem. Engrs., (Supplement) **32**, S 6 (1954).
5) Hatch, T. F. and R. L. Pigford: Ind. Eng. Chem. Fundamentals, **1**, 209 (1962).
6) International Critical Tables, Vol. **5**, 62 (1928).
7) "Kagaku Benran", p. 572 (1958), Maruzen Co. Ltd.
8) Matsuyama, T.: Chem. Eng. (Japan), **14**, 245 (1950).
9) Nijsing, R. A. O., R. H. Hindriksz and H. Kramers: Chem. Eng. Sci., **10**, 88 (1959).
10) Onda, K., T. Okamoto and Y. Yamaji: Chim. Eng. (Japan), **24**, 918 (1960).
11) "Perry's Hand Book", 4th ed., p. 14-4 (1964), McGraw Hill.
12) *ibid*, p. 14-25.
13) *ibid*, p. 14-26.
14) Raimonde, P. and H. L. Toor: A. I. Ch. E. Journal, **5**, 86 (1959).
15) Rehm, T. R., A. J. Moll and A. L. Babb: A. I. Ch. E. Journal, **9**, 760 (1963).
16) Reid, R. C. and T. K. Sherwood: "The Properties of Gases and Liquids", p. 268 (1958), McGraw Hill.
17) *ibid*, p. 275.
18) Vielstich, W.: Chem. Ing. Techn., **28**, 543 (1956).